

First-order liquid-hexatic phase transition in hard disks

Etienne P. Bernard & Werner Krauth

Laboratoire de physique statistique, Ecole normale supérieure, UPMC, Université Paris Diderot, CNRS, 24 rue Lhomond, 75231 Paris Cedex 05, France

The hard-disk model has exerted outstanding influence on computational physics and statistical mechanics. Decades ago, hard disks were the first system to be studied by Markov-chain Monte Carlo methods¹ and by molecular dynamics². It was in hard disks, through numerical simulations, that a two-dimensional melting transition was first seen to occur³ even though such systems cannot develop long-range crystalline order⁴. Scores of theoretical, computational, and experimental works have analysed this fundamental melting transition, without being able to settle its nature. The first-order melting scenario between a liquid and a solid (as in three dimensions⁵), and the Kosterlitz, Thouless⁶, Halperin, Nelson⁷ and Young⁸ (KTHNY) scenario with an intermediate hexatic phase separated by continuous transitions from the liquid and the solid have been mainly focussed upon^{9,10,11,12,13,14}. Here we show by large-scale simulations using the powerful Event-chain Monte Carlo algorithm¹⁵ that the hard-disk system indeed possesses a narrow hexatic phase, where orientational order is maintained across large samples while positional order is short-ranged. However, in difference with the KTHNY scenario, the liquid-hexatic phase transition is proven to be first-order. In simulations at fixed volume and number of disks, we identify a two-phase region, where the liquid with large but finite orientational correlation length coexists with the hexatic. At higher densities, we reach the pure hexatic phase, and then witness the transition into the solid phase characterised by quasi-long range positional order. Our work closes a crucial gap in the understanding of one of the fundamental models in statistical physics, which is at the basis of a large body of theoretical and experimental work in films, suspensions, and other condensed-matter systems^{16,17}.

The hard-disk liquid, at low density, is well described by effective theories¹⁸, and easily simulated because of its essentially local nature. Correlations build up on larger length scales as the density increases, both for the positions and the orientations. To define the latter, we establish the neighbours for each disk k by the Voronoi construction. We then compute the local orientation $\Psi_k = \langle \exp(6i\varphi_{kl}) \rangle$, averaged over neighbours l , with φ_{kl} the angle of the bond between the centres of k and l and a fixed axis. The absolute value of Ψ_k is equal to one if k and its neighbours are arranged as in a triangular lattice. The sample orientation $\Psi = 1/N \sum_k \Psi_k$ averages the local orientations over the N disks in the sample.

In a window of densities (packing fractions) between $\eta=0.700$ and $\eta=0.716$, where previous computations did not reach thermal equilibrium for large systems^{13,14}, we witness the coexistence of a liquid with a phase of higher density which preserves orientational order across the entire system (see fig. 1a-c). We will identify this phase as a hexatic because of its short-range positional order along with (quasi) long-range orientational order. The two-phase nature of the system at densities between 0.700 and 0.716 is well captured by the bi-modality of its coarse-grained density distribution whose peak positions correspond approximately to the two limiting densities (see fig. 1e), while the peak heights adjust to the given total packing fraction.

The limiting densities of the coexistence region are obtained with better precision than in fig. 1e by the Maxwell construction of the virial pressure P as a function of density (see fig. 2a). The approximate $1/\sqrt{N}$ scaling for the separation ΔP of the local maximum and minimum in the pressure curve is compatible with the \sqrt{N} free-energy scaling of a smooth interface in two dimensions¹⁹ (see fig. 2b). Rather than analysing the individual phases in the coexistence region [0.700, 0.716], we study the pure-phase systems just outside this region, which show the same bulk properties and correlation functions, but are free of the complications arising from the interface (see figs 2c and 2d). To measure the positional order in the high-density phase (see fig 2d), we consider the structure factor

$\mathbf{S}(\mathbf{k})=1+N/V\int d\mathbf{r} (g(\mathbf{r})-1)\exp(i\mathbf{k}\mathbf{r})$, where $g(\mathbf{r})$ is the two-dimensional pair correlation function, averaged over samples oriented with respect to Ψ . We then compute the positional correlation function through $C_k(r)=\int d\phi g(r,\phi)\exp(i\mathbf{k}\mathbf{r})/\int d\phi g(r,\phi)$, where \mathbf{k} is at the empirically obtained peak value of \mathbf{S} , \mathbf{k}_{peak} . Earlier workers^{14,20} approximated \mathbf{k}_{peak} by \mathbf{k}_{perf} , the reciprocal vector of the perfect triangular lattice, and severely under-estimated the positional order (see fig. 2e).

The positional correlation function just above the coexistence region decays exponentially (see fig. 3a) in the presence of extremely slowly decaying orientational correlations (see fig. 3b). This characterizes the high-density coexisting phase in fig 2d as a hexatic. In contrast, the low-density coexisting phase is a liquid because of its short-range orientational order (see fig 3c). Together, the phase transition is thus first-order liquid-hexatic. In the hexatic, the positional correlation length increases rapidly with density. The positional correlation function eventually becomes algebraic with an exponent close to -1/3 as in the KTHNY scenario (see fig 3d). We estimate the hexatic-solid transition to take place around $\eta=0.720$.

The event-chain algorithm used in our studies is about two orders of magnitude faster (in CPU time) than the local Monte Carlo. This speed-up allows us to reach equilibrium for $1,024^2$ disks. As an illustration of convergence, and a proof that hard disks in the window of densities $[0.700,0.716]$ are indeed phase-separated, we have simulated our largest systems after quenches from radically different initial conditions, namely the crystal, with $|\Psi|=1$, and the liquid, for which $|\Psi|$ vanishes. In both cases (see fig. 4a and b), a slow process of coarsening leads to phase separation, yielding configurations with similar values of the sample-orientation modulus after $t\sim 10^6$ displacements per disk (see fig. 4c). Many earlier calculations either considered system sizes which were not clearly above the inherent length scales of this problem or used insufficient simulation times, for which phase separation has not completed. Our production runs for $N=1,024^2$ were obtained from Markov chains with total running times 30 times larger than those shown in fig. 4a and b .

Low-dimensional physics is an extremely active field of research which thrives on the multitude of phenomena made possible by strong fluctuations, hidden length scales, generic algebraic correlations and absence of strong universality, among others. These ingredients, together with the lack of powerful numerical methods in the past, have made the hard-disk problem rich and difficult. We expect future theoretical and experimental research to build on our clear-cut solution of this problem, and to further investigate, for example, the 2d-3d cross-over¹⁷, dynamics, and the expected dependence of the transition scenario on the underlying microscopic model²¹.

References

- ¹Metropolis, N., Rosenbluth, A. W., Rosenbluth, M. N., Teller, A. H. & Teller, E. Equation of state calculations by fast computing machines. *J. Chem. Phys.* **21** 1087 (1953).
- ²Alder, B. & Wainwright, T. E. Phase transition for a hard sphere system. *J. Chem. Phys.* **27** 1208 (1957).
- ³Alder, B. J. & Wainwright, T. E. Phase transition in elastic disks. *Phys. Rev.* **127**, 359 (1962)
- ⁴Mermin, N. D. & Wagner, H. Absence of ferromagnetism or antiferromagnetism in one- or two-dimensional isotropic Heisenberg models. *Phys. Rev. Lett.* **17**, 1133 (1966).
- ⁵Hoover, W. G. & Ree, F. H. Melting transition and communal entropy for hard spheres. *J. Chem. Phys.* **49**, 3609 (1968).
- ⁶Kosterlitz, J. M. & Thouless, D. J. Ordering, metastability and phase transitions in 2 dimensional systems. *J. Phys. C* **6**, 1181 (1973).
- ⁷Halperin, B. I. & Nelson, D. R. Theory of 2-dimensional melting. *Phys. Rev. Lett.* **41**, 121 (1978).
- ⁸Young, A. P. Melting and the Coulomb gas in 2 dimensions. *Phys. Rev.* **B 19**, 1855 (1979).
- ⁹Strandburg, K. J. Two-dimensional melting. *Rev. Mod. Phys.* **60**, 161 (1988).
- ¹⁰Lee, J. Y. & Strandburg, K. J. 1st-order melting transition of the hard-disk system. *Phys. Rev. B* **46**,

11190 (1992).

¹¹Zollweg, J. A. & Chester, G. V. Melting in 2 dimensions. *Phys. Rev. B* **46**, 11186 (1992).

¹²Weber, H., Marx, D. & Binder, K. Melting transition in 2 dimensions – a finite-size-scaling analysis of bond-orientational order in hard disks. *Phys. Rev. B* **51** 14636 (1995).

¹³Jaster, A. The hexatic phase of the two-dimensional hard disk system. *Phys. Lett. A* **330**, 120 (2004).

¹⁴Mak, C. H. Large-scale simulations of the two-dimensional melting of hard disks. *Phys. Rev. E* **73**, 065104(R) (2006).

¹⁵Bernard, E. P., Krauth, W. & Wilson, D. B. Event-chain Monte Carlo algorithms for hard-sphere systems. *Phys. Rev. E* **80** 056704 (2009).

¹⁶Zahn, K., Lenke, R. & Maret, G. Two-Stage Melting of Paramagnetic Colloidal Crystals in Two Dimensions. *Phys. Rev. Lett.* **82**, 2721 (1999).

¹⁷Peng, Y., Wang Z., Alsayed, A. M., Yodh, A. G. & Han Y. Melting of Colloidal Crystal Films. *Phys. Rev. Lett.* **104**, 205703 (2010).

¹⁸Hansen, J.-P. & McDonald I. R. *Theory of Simple Liquids*, 3rd edition (Academic Press) (2006).

¹⁹Lee, J. & Kosterlitz, J. M. New numerical method to study phase transitions. *Phys. Rev. Lett.* **65**, 137 (1990).

²⁰Bagchi, K., Andersen, H. C. & Swope, W. Computer simulation study of the melting transition in two dimensions *Phys. Rev. Lett.* **76** 255 (1996).

²¹van Enter, A. C. D. & Shlosman S. B. First-order transitions for n-vector models in two and more dimensions: rigorous proof. *Phys. Rev. Lett.* **89** 285702 (2002).

Author contributions Both authors collaborated closely in all aspects of this study.

Correspondence Correspondence and requests for materials should be addressed to W.K. (email: werner.krauth@ens.fr).

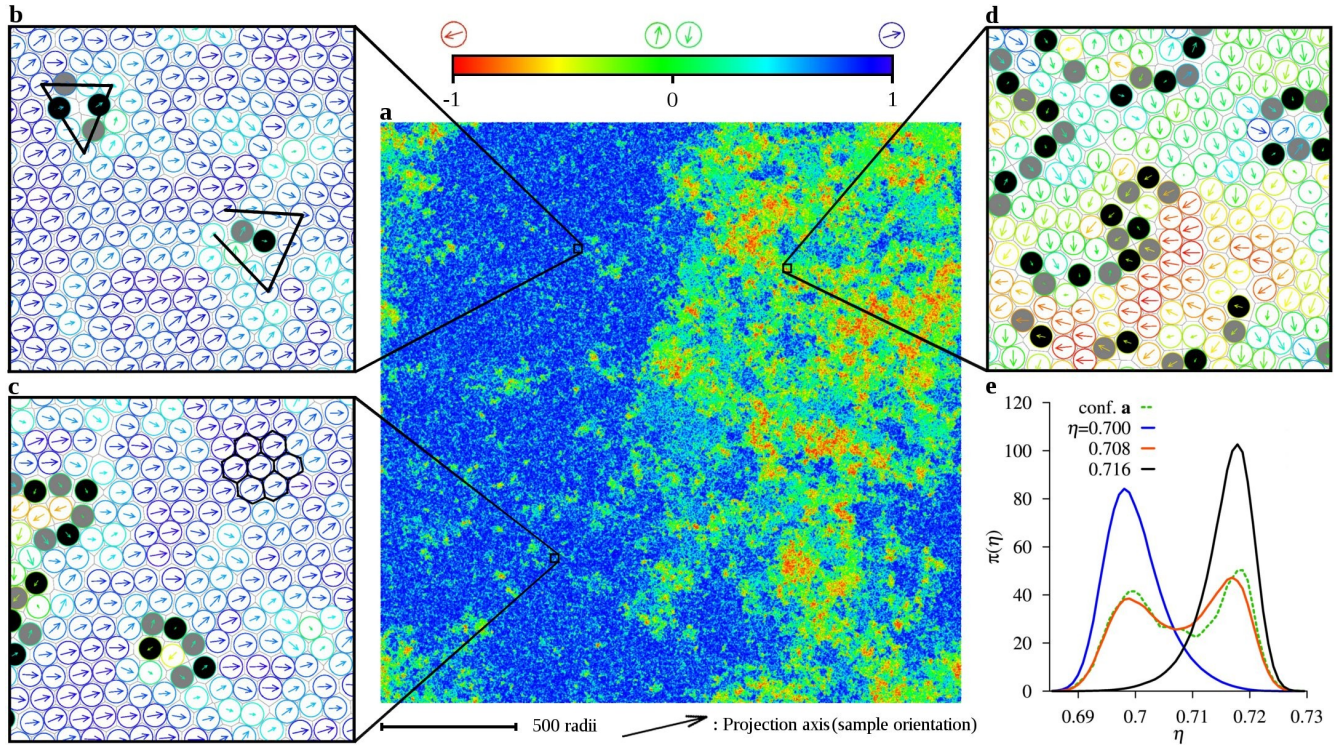


Fig. 1 Liquid-hexatic coexistence in an equilibrated sample of $N=1,024^2$ disks with radius σ at packing fraction $\eta=N\pi\sigma^2/V=0.708$ in a square box of volume V with periodic boundary conditions. **a**: Projection of the local orientation Ψ_k onto the sample orientation Ψ , showing (quasi) long-range orientational correlations in the hexatic phase (blue area, to the left) and short-range correlations in the liquid (to the right). **b** and **c**: Detailed views in the dense (hexatic) phase. The arrow inside disk k describes Ψ_k . An isolated dislocation, composed of a disk with five neighbours (in grey) and one with seven neighbours (in black), is shown. **d**: Detailed view in the liquid phase, with uncorrelated local orientations above a scale of $\sim 100\sigma$. **e**: Bi-modal density distribution, coarse-grained over a radius of 50σ around each disk, for the sample in **a** (green dotted line), and averaged over samples at $\eta=0.708$ (red), compared to the uni-modal distributions at $\eta=0.700$ (blue) and $\eta=0.716$ (black).

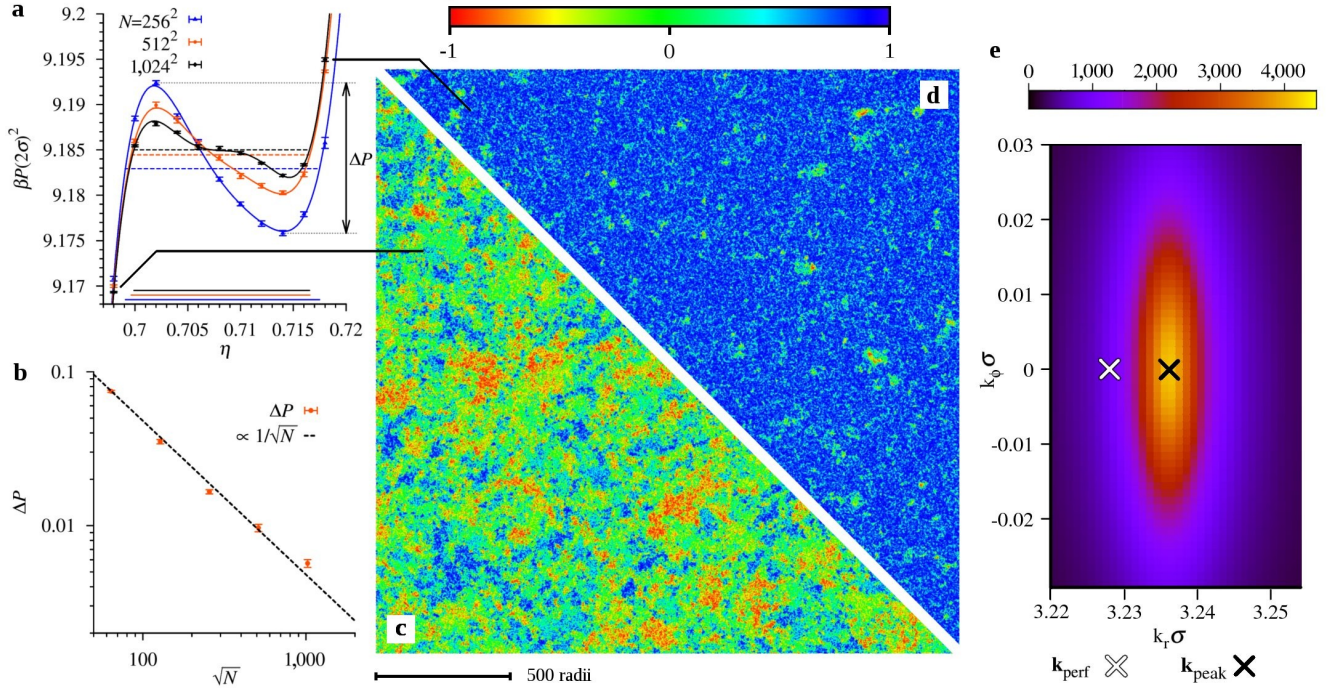


Fig. 2 Coexistence region and limiting densities for hard disks. **a:** Equation of state and Maxwell construction for different system sizes. Statistical errors were computed as follows (example for $N=1,024^2$): 64 independent equilibrium configurations, obtained from a single event-chain calculation with 6×10^7 displacements per disk, served as starting points of independent runs. Gaussian error from these runs is indicated. **b:** Pressure difference ΔP , showing expected $1/\sqrt{N}$ scaling. **c** and **d:** Equilibrated samples of $1,024^2$ hard disks at $\eta=0.698$ (*lower triangle*, half of sample shown) and $\eta=0.718$ (*upper triangle*) (Projection of Ψ_k onto Ψ and colour code as in fig. 1). **e:** Configuration-averaged structure factor $S(\mathbf{k})$ (one of the six first Bragg peaks) at $\eta=0.718$. Positional correlation functions must be computed at the peak value \mathbf{k}_{peak} of S . The reciprocal vector of the perfect triangular lattice \mathbf{k}_{perf} (white cross) used by earlier workers neglects the modification of the lattice spacing due to defects.

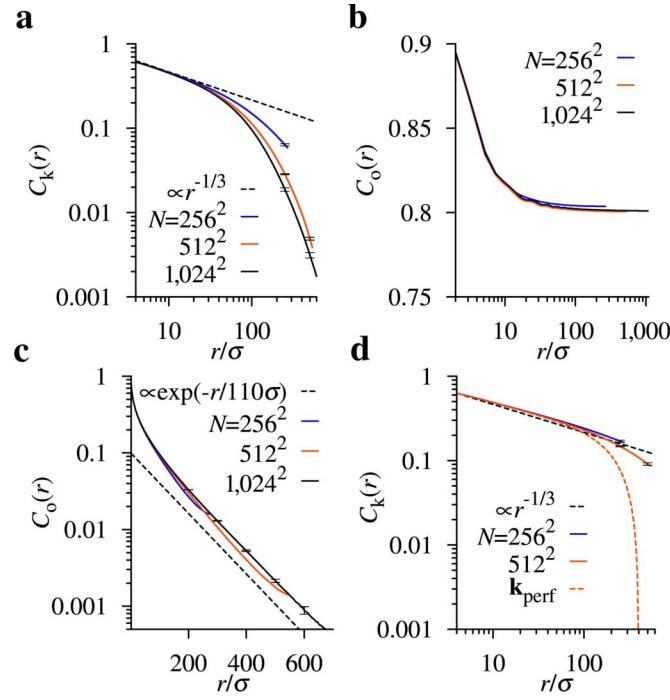


Fig. 3 Pure-phase orientational and positional correlation functions. **a** and **b**: Exponentially decaying positional correlations and (quasi)-long-range orientational correlations at $\eta=0.718$, in the hexatic phase. **c**: Exponentially decaying orientational correlation functions at $\eta=0.700$, the lower boundary of the coexistence region. **d**: Positional correlations at $\eta=0.720$, compatible with an $\propto r^{-1/3}$ algebraic decay. The correlation function at \mathbf{k}_{perf} decays much faster. Statistical errors were determined as in fig. 2. The bare correlation functions were averaged over a Gaussian kernel of a few radii.

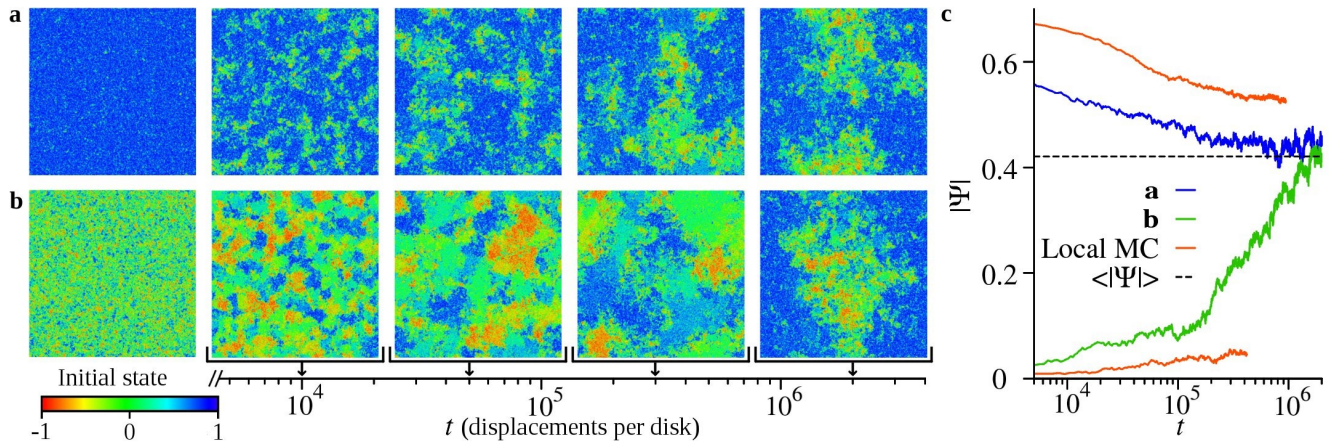


Fig. 4 Approach to equilibrium from different initial conditions. **a** and **b**: Systems with $1,024^2$ disks at density 0.708, after a quench from a high-density crystal (**a**) and from a low-density liquid (**b**), showing coarsening followed by phase separation (Projection of Ψ_k onto Ψ and colour code as in figs 1 and 2). Each of the runs takes one week of computer time. **c**: Absolute value of the sample orientation for the simulations in **a** and **b**, compared to runs with the local Monte Carlo algorithm from the same initial conditions (time in attempted displacements per disk), which has not yet reached equilibrium. The correlation time of the event-chain algorithm, on the order of 10^6 displacements per disk, estimated from **c**, agrees with the analysis of the auto-correlation function of $|\Psi|$ in the production runs for figs 2 and 3, with 6×10^7 displacements per disk.